RSC Advances

RSC Publishing

PAPER

View Article Online
View Journal | View Issue

Field emission performance of hierarchical ZnO nanocombs

Cite this: *RSC Adv.*, 2013, **3**, 26149

C. L. Liu,[a] H. Gao,*[a] L. Li,*[a] X. Liu,[a] Q. Gao,[a] H. X. Cuo,[a] T. T. Chen[a] and G. Q. Miao[b]

Received 17th July 2013
Accepted 4th October 2013

DOI: 10.1039/c3ra43538e

www.rsc.org/advances

Hierarchical ZnO nanocombs (ZnO NCs) with a high field enhancement factor were synthesized on Si substrates by the chemical vapor deposition method. The X-ray diffraction (XRD) pattern indicates that ZnO NCs have a hexagonal wurtzite structure. Electric field emission (FE) from hierarchical ZnO NCs was realized. The turn-on field was measured to be 3.6 V μm^{-1}, and the field enhancement factor of the hierarchical ZnO NCs was estimated to be 3490. The high field enhancement factor is derived from the special morphology of the product. This kind of hierarchical ZnO NCs has a great potential for field emission displays.

Introduction

Nanomaterials are not only at the cutting edge of the research into materials nowadays, but are also gradually blending in with our daily lives.[1,2] One-dimensional nanomaterials have received much attention due to their promising applications in devices. As one of the most important multifunctional semiconductor materials, ZnO, with a wide band gap of 3.37 eV and large exciton binding energy (60 meV) at room temperature, has been shown to have a wide range of applications in optoelectronic, electronic, and electromechanical devices, for instance, in light-emitting diodes,[3] solar cells,[4] ultraviolet lasers,[5] nano-generator,[6] and field emission devices.[7] FE (field emission) is one of the main features of nanomaterials, and is of huge commercial interests in electronic devices. Field emission, which is called the Fowler–Nordheim tunneling, is a form of quantum tunneling in which electrons pass from an emitting material performing as the cathode to the anode through a vacuum chamber driven by a high electric field.[8] ZnO nanomaterials have attracted great attention as a field emitter due to their high aspect ratio and high mechanical stability. The special morphology of one-dimensional nanomaterials has already shown great advantages in field emission devices.[9] In recent years, ZnO nanorods,[10] nanopins,[11] nanoneedles,[12] and nanotubes[13] were synthesized, and their FE performances have been reported. However, there are some challenges to improve FE performances of ZnO nanomaterials, such as how to further improve the field enhancement factor, increase the aspect ratio and decrease the density of the emitter geometry. In this paper, the high aspect ratio and low-density hierarchical ZnO NCs were synthesized and the FE performances of the product were measured. The field enhancement factor was determined to be about 3490.

Experimental

The hierarchical ZnO NCs and ZnO nanowires (ZnO NWs) were synthesized by the chemical vapor deposition method (CVD). The ZnO powders were loaded into one end of an alumina boat. The Si substrate (0.5 cm $\times$ 0.8 cm) was cleaned for 5 minutes in an ultrasonic bath with acetone, ethanol and deionized water, respectively. The Au films were deposited on the Si substrates by the vacuum ion sputtering method. The Si substrates were placed downstream of the precursor. The boat was placed inside an alumina tube inserted into a horizontal furnace. Nitrogen gas was introduced into the system as the carrier gas with a constant flow rate of 50 sccm, and the working pressure was kept at 500 Pa. The furnace was heated to a preset temperature (1300 °C) and maintained at this temperature for one hour. Then the furnace was cooled down to room temperature naturally. The only difference in the two products is the temperature of the substrate. In this experiment, the distance between the source and the hierarchical ZnO NCs is 18 cm and the distance of ZnO NWs is longer.

The morphology and the crystal structure of the synthesized-products were characterized by the field-emission scanning electron microscopy (FE-SEM; S-4800, Hitachi, Japan), the transmission electron microscopy (TEM; FEI, Tecnai TF20), and the XRD (D/max2600, Rigaku, Japan). Photoluminescence spectra (PL) of the samples were characterized by the Micro-Raman spectrometer (J-Y; HR800, France) under the excitation wavelength of 325 nm. FE properties were characterized with a two-parallel-plate equipment in a vacuum chamber with a

[a]*Key Laboratory of Photonic and Electronic Bandgap Materials of Ministry of Education, School of Physics and Electronic Engineering, Harbin Normal University, Harbin 150025, People's Republic of China. E-mail: gaohong65cn@126.com; physics_lin@hotmail.com*

[b]*Key Laboratory of Excited State Processes, Changchun Institute of Optics, Fine Mechanics and Physics, Chinese Academy of Sciences, 16-East South Lake Road, Changchun 130021, People's Republic of China*

pressure of 1.0×10^{-4} Pa. The samples on the Si substrate were used as the cathode and a piece of glass coated with the ITO thin film played the role of an anode. The distance between two electrodes was 125 μm. All of the experiments were made at room temperature.

Results and discussion

Fig. 1(a) shows the low-magnification SEM image of the hierarchical ZnO NCs. It can be seen that a large number of hierarchical ZnO NCs were uniformly grown on the silicon substrate. The high-magnification SEM image of a representative nanocomb with fine nanowire branches grown on one side of the nanoribbons is shown in Fig. 1(b). It can be clearly seen from Fig. 1(b) that three parts are contained in the nanocomb structure: the ribbon, the transition zone from ribbon to branches, and the branches. The nanostructure abruptly sharpens from the transition zone to the branches. The transition zone is about 100 nm in width, and the diameter of the branches is about 20 nm, respectively. As shown in Fig. 1(c) and (a), a large number of uniform size ZnO NWs grew on the substrate. Fig. 1(d) shows that the ZnO NWs have an average diameter of 200 nm. Fig. 2(a) and (c) are low-magnification TEM images of typical hierarchical ZnO NCs and ZnO NWs. We cannot see long nanowires in the nanocombs owing to the fact that they were so fine that they broke when sampled. Fig. 2(b) and (d) are the corresponding high-resolution TEM images of the ZnO nanomaterials. An amorphous carbon film was coated on the two kinds of ZnO nanomaterials, and the thickness of carbon film is about 2 nm for the nanocombs and 7 nm for the nanowires, respectively. The carbon comes from CO_2 in the air.[14] The crystalline quality of the hierarchical ZnO NCs is much better than that of the ZnO NWs. Fig. 3 shows the XRD patterns of the two kinds of ZnO nanomaterials. From the XRD analysis, the great majority of diffraction peaks in this pattern belong to the hexagonal wurtzite structure of ZnO (JCPDS card no. 36-1451). Here the peaks marked (111) and (200) come from the Si substrate (JCPDS card no. 04-0784) and the Au film

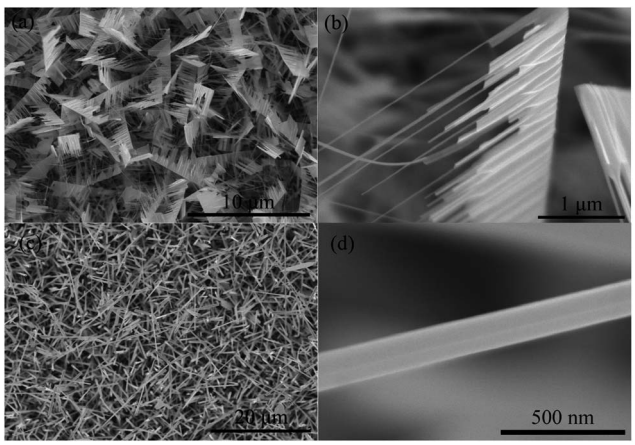

Fig. 1 (a) and (c) Low-magnification SEM images of the hierarchical ZnO NCs and ZnO NWs, respectively. (b) and (d) High-magnification SEM images of the hierarchical ZnO NCs and ZnO NWs, respectively.

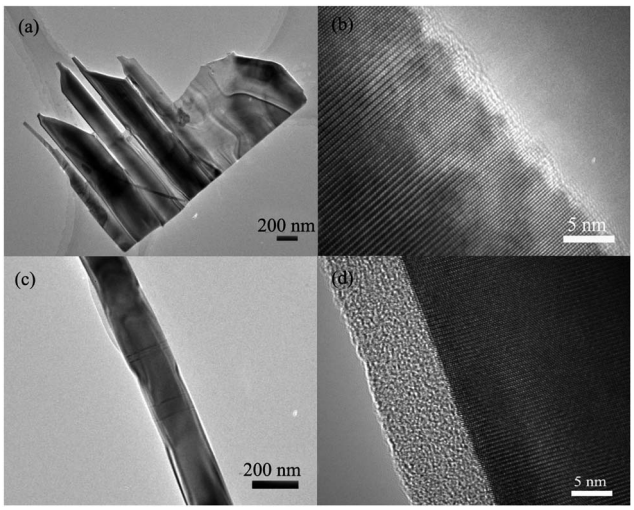

Fig. 2 (a) and (c) Low-magnification TEM images of the hierarchical ZnO NCs and ZnO NWs, respectively. (b) and (d) High-magnification TEM images of the hierarchical ZnO NCs and ZnO NWs, respectively.

(JCPDS card no. 79-0205). The diffraction peaks of no other phases can be found in the XRD spectra. This indicates that the two synthesized ZnO nanomaterials are single-crystalline structures. In Fig. 4, the PL spectra of the two ZnO nanomaterials show an ultraviolet (UV) emission peak at 381 nm and a green light emission that is really intense. It is known that the UV peak arises from the near band-edge exciton recombination, and the green emission comes from the intrinsic defects.[15] So, the PL spectrum implies that the crystal quality of the hierarchical ZnO NCs is superior to that of the ZnO NWs. Fig. 5 shows the field emission current densities *vs.* electric field characteristics of the two ZnO nanomaterials between the cathode and the anode. The emission current densities enhance rapidly with the electric field and no current equilibration is observed. The turn-on electric fields (E_{to}) of the hierarchical ZnO NCs and ZnO NWs are about 3.6 V μm^{-1} and 3.1 V μm^{-1} at 1 μA cm^{-2} current density, respectively. A strong visible emission peak of the ZnO NWs is observable in Fig. 4. This peak clearly indicates the presence of intrinsic defects, while the intrinsic defects result in

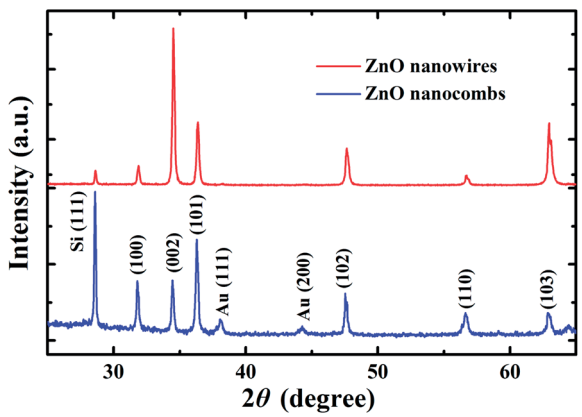

Fig. 3 XRD patterns of the hierarchical ZnO NCs and ZnO NWs.

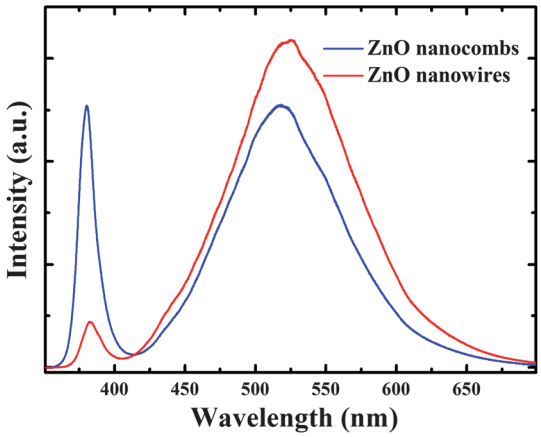

Fig. 4 PL spectra of the hierarchical ZnO NCs and ZnO NWs.

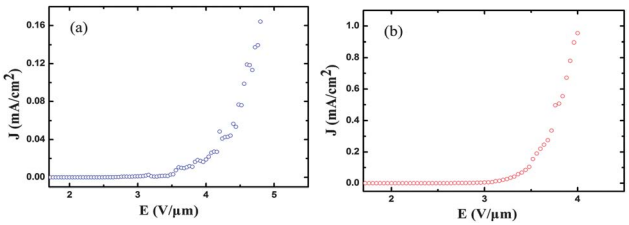

Fig. 5 (a) and (b) The *J*–*E* characteristic curves of field emission from the hierarchical ZnO NCs and ZnO NWs, respectively.

the increase of carrier concentration, and as a consequence, reduce the resistance of the nanowires, thus obtaining a low turn-on field relative to the ZnO NCs. Furthermore, the thick amorphous carbon films are also helpful to decrease the turn-on field.[16,17]

The relationship between the field emission current densities (J) and electric field (E) is further analyzed according to the Fowler–Nordheim equation:[10]

$$J = (A\beta^2E^2/\phi)\exp(-B\phi^{3/2}/\beta E),$$

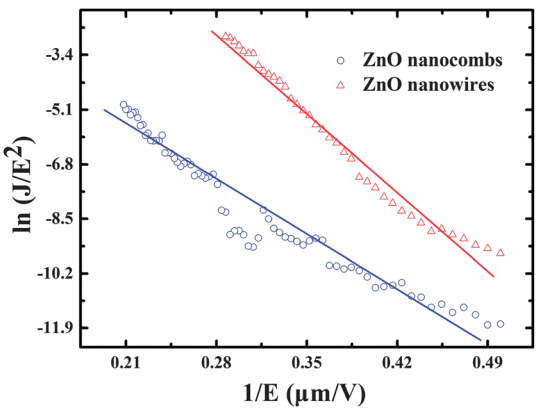

Fig. 6 The corresponding $\ln(J/E^2)$–$1/E$ plot of the hierarchical ZnO NCs and ZnO NWs.

Table 1 FE data from the hierarchical ZnO NCs and other ZnO materials

Materials	E_{to} (V μm^{-1})	Factor
Hierarchical ZnO NCs	3.6	3490
ZnO nanotower with a small crown[9]	4.5	2100
Hierarchical ZnO hexagonal towers[19]	2.37	2691
Hierarchical-structure ZnO[20]	4.8	3400
Six-fold-symmetrical hierarchical ZnO[21]	5.6	1351
AlZnO nanowire arrays[22]	3.9	1315
ZnO nanorod arrays[10]	2	1680
Aligned ultralong ZnO nanobelts[23]	1.3	1.4×10^4

where A and B are constants with $A = 1.54 \times 10^{-6}$ A eV V^{-2} and $B = 6.83 \times 10^3$ eV$^{-3/2}$ V μm^{-1}), ϕ is the work function of the emitting materials,[18] and β is a primary parameter to describe the field enhancement, named the field enhancement factor. Fig. 6 plots $\ln(J/E^2)$ *versus* $1/E$. A linear relation between J/E^2 and $1/E$ is obvious. From this figure and the above equation, one can derive the field enhancement factors of the hierarchical ZnO NCs and ZnO NWs to be 3490 and 1625, respectively, by taking the work function to be 5.3 eV. To the best of our knowledge, the field enhancement factor of the ZnO NCs is higher than most of those of the ZnO nanomaterials reported in the literature, as shown in Table 1.

The field enhancement factor is defined as the real value of the electric field at the apex compared to its average macroscopic value.[7] It is a primary parameter to judge the performance of FE. This parameter is bound up with many factors. First, the specific geometry plays an important role in enhancing the field enhancement factor. The emission current converges to the place of sharp tips. ZnO NCs with a hierarchical structure lead to the electrons to be quickly centralized and to emit into the vacuum more easily. Thus, a high field enhancement factor is ensured.[9] In addition, the specific transition zone reduces the distance between the emitters, and decreases the screening effect to enhance the field emission factor.[24] Second, it is known that the field enhancement factor of an individual emitter is approximately proportional to the aspect ratio h/r, where h and r are the length and radius of the emitter. The field enhancement factor will be enhanced by decreasing the radius of curvature and increasing the height of the emitting center. In this work, h is about 7 μm and r is in the range of 20 nm, and therefore hierarchical ZnO NCs have a very high field enhancement factor among ZnO nanomaterials.[23] Third, the good crystal quality of the ZnO NCs can also enhance the field enhancement factor.[25] In short, the specific geometry, the aspect ratio and the crystal quality contribute to improvement of the field enhancement factor of the hierarchical ZnO NCs. However, the increase of field enhancement factor may be mainly attributed to the specific morphological structure of the emitters.

Conclusion

In summary, the single-crystalline hierarchical ZnO NCs and ZnO NWs were synthesized by the chemical vapour deposition

method on a Si substrate at 1300 °C. The FE performances were measured. A high field enhancement factor of 3490 was obtained for the hierarchical ZnO NCs. Such a result is attributed to the specific geometry. Obviously, the hierarchical ZnO NCs are good candidates for FE devices.

Acknowledgements

This work was partially supported by the Natural Science Foundation of China (nos 11074060, 51172058, and 51102069), the Key Project of the Science Technology and Research Project of Education Bureau, Heilongjiang Province (12521z012), and the Graduate Students' Scientific Research Innovation Project of Heilongjiang Province (2013).

References

1 M. H. Huang, S. Mao, H. Feick, H. Q. Yan, Y. Y. Wu, K. Hannes, E. Weber, R. Russo and P. D. Yang, *Science*, 2001, **292**, 8.
2 Ü. Özgür, Ya. I. Alivov, C. Liu, A. Teke, M. A. Reshchikov, S. Doğan, V. Avrutin, S. J. Cho and H. Morkoc, *J. Appl. Phys.*, 2005, **98**, 041301.
3 Ya. I. Alivov, E. V. Kalinina, A. E. Cherenkov, D. C. Look and B. M. Ataev, *Appl. Phys. Lett.*, 2003, **83**, 4719.
4 K. Keis, E. Magnusson, H. Lindstrom, S. E. Lindquist and A. Hagfeldt, *Sol. Energy Mater. Sol. Cells*, 2002, **73**, 51–58.
5 Z. K. Tang, G. K. L. Wong, P. Yu, M. Kawasaki, A. Ohtomo, H. Koinuma and Y. Segawa, *Appl. Phys. Lett.*, 1998, **72**, 3270.
6 Z. H. Lin, Y. Yang, J. M. Wu, Y. Liu, F. Zhang and Z. L. Wang, *J. Phys. Chem. Lett.*, 2012, **3**, 3599–3604.
7 J. Xiao, X. X. Zhang and G. M. Zhang, *Nanotechnology*, 2008, **19**, 295–706.
8 X. S. Fang, Y. Bando, U. K. Gautam, C. H. Ye and D. Golberg, *J. Mater. Chem.*, 2008, **18**, 509–522.
9 N. Pan, H. Z. Xue, M. H. Yu, X. F. Cui, X. P. Wang, J. G. Hou, J. X. Huang and S. Z. Deng, *Nanotechnology*, 2010, **21**, 225–707.
10 H. Zhang, D. R. Yang, X. Y. Ma and D. L. Que, *J. Phys. Chem. B*, 2005, **109**, 36.
11 C. X. Xu and X. W. Sun, *Appl. Phys. Lett.*, 2003, **83**, 3806.
12 C. J. Park, D. K. Choi, J. Yoo, G. C. Yi and C. J. Lee, *Appl. Phys. Lett.*, 2007, **90**, 083107.
13 A. Wei, X. W. Sun, C. X. Xu, Z. L. Dong, M. B. Yu and W. Huang, *Appl. Phys. Lett.*, 2006, **88**, 213102.
14 K. W. Kwong and Q. Li, *J. Appl. Phys.*, 2005, **98**, 024301.
15 Y. Li, G. W. Meng, L. D. Zhang and F. Phillipp, *Appl. Phys. Lett.*, 2000, **76**, 15.
16 W. Zhu, C. Bowe, O. Zhou, G. Kochanski and S. Jin, *Appl. Phys. Lett.*, 2009, **75**, 6.
17 H. Murakami, M. Hirakawa, C. Tanaka and H. Yamakawa, *Appl. Phys. Lett.*, 2000, **76**, 13.
18 R. Maity, A. N. Banerjee and K. K. Chattopadhyay, *Appl. Surf. Sci.*, 2004, **236**, 231.
19 P. Wang, X. T. Zhang, J. Wen, L. L. Wu, H. Gao, E. Zhang and G. Q. Miao, *J. Alloys Compd.*, 2012, **533**, 88–92.
20 Y. X. Liu, Y. Z. Xie, J. T. Chen, J. Liu, C. T. Gao, C. Yun, B. A. Lu and E. Q. Xie, *J. Am. Ceram. Soc.*, 2011, **94**, 4387–4390.
21 Z. Q. Wang, J. F. Gong, Y. Su, Y. W. Jiang and S. G. Yang, *Cryst. Growth Des.*, 2010, **10**, 2455.
22 X. Y. Xue, L. M. Li, H. C. Yu, Y. J. Chen, Y. G. Wang and T. H. Wang, *Appl. Phys. Lett.*, 2006, **89**, 043118.
23 W. Z. Wang, B. Q. Zeng, J. Yang, B. Poudel, J. Y. Huang, M. J. Naughton and Z. F. Ren, *Adv. Mater.*, 2006, **18**, 3275–3278.
24 X. D. Wang, J. Zhou, C. S. Lao, J. H. Song, N. S. Xu and Z. L. Wang, *Adv. Mater.*, 2007, **19**, 1627–1631.
25 H. Kim, S. Jeon, M. Lee, J. Lee and K. Yong, *J. Mater. Chem.*, 2011, **21**, 13458–13463.

